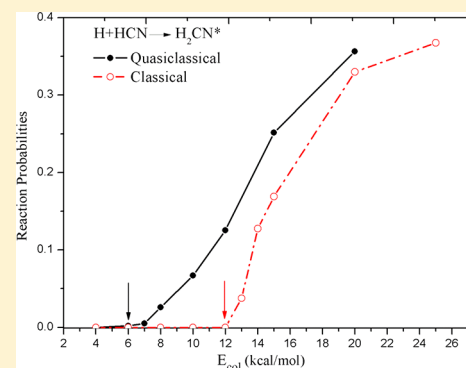


Zero-point Energy is Needed in Molecular Dynamics Calculations to Access the Saddle Point for $\text{H}+\text{HCN}\rightarrow\text{H}_2\text{CN}^*$ and *cis/trans*- HCNH^* on a New Potential Energy Surface

Xiaohong Wang and Joel M. Bowman*

Cherry L. Emerson Center for Scientific Computation and Department of Chemistry, Emory University, Atlanta, Georgia 30322, United States

ABSTRACT: We calculate the probabilities for the association reactions $\text{H}+\text{HCN}\rightarrow\text{H}_2\text{CN}^*$ and *cis/trans*- HCNH^* , using quasiclassical trajectory (QCT) and classical trajectory (CT) calculations, on a new global ab initio potential energy surface (PES) for H_2CN including the reaction channels. The surface is a linear least-squares fit of roughly 60 000 CCSD(T)-F12b/aug-cc-pVDZ electronic energies, using a permutationally invariant basis with Morse-type variables. The reaction probabilities are obtained at a variety of collision energies and impact parameters. Large differences in the threshold energies in the two types of dynamics calculations are traced to the absence of zero-point energy in the CT calculations. We argue that the QCT threshold energy is the realistic one. In addition, trajectories find a direct pathway to *trans*- HCNH , even though there is no obvious transition state (TS) for this pathway. Instead the saddle point (SP) for the addition to *cis*- HCNH is evidently also the TS for direct formation of *trans*- HCNH .



I. INTRODUCTION

The H_2CN system has attracted wide interest, especially the reaction $\text{H}_2 + \text{CN} \rightarrow \text{H} + \text{HCN}$. There have been numerous theoretical studies of both the potential and dynamics, including classical and quantum calculations.^{1–19} The construction of an accurate potential energy surface is essential to study the reaction dynamics. There are several potential energy surfaces (PESs) for the H_2CN system. Sun and Bowman³ reported a limited, semiempirical PES based on ab initio calculations of the saddle points. Reduced dimensionality quantum reactive scattering calculations for $\text{H}_2 + \text{CN} \leftrightarrow \text{H} + \text{HCN}$ were done with this PES, which does not describe the formation of the CNH_2 complex and $\text{H} + \text{HNC}$ fragments. In a later study, Horst et al.⁵ carried out multireference configuration interaction (MRCI) calculations and constructed a global PES, using many-body expansion. Based on the PES, they studied the $\text{H}_2 + \text{CN}$ reaction dynamics in detail using QCT calculations. Later, Sumathi and Nguyen⁶ reported a study of the doublet and quartet PESs, which covered more stationary points for these states using CCSD(T) method with a 6-311++G(d,p) basis. They noted some quantitative differences with the earlier Horst et al. doublet PES. Rate constants of various addition reactions were determined using QRRK theory.

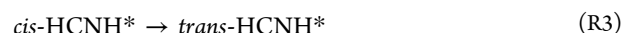
Previous dynamics studies were mainly focused on the reaction $\text{H}_2 + \text{CN} \rightarrow \text{H} + \text{HCN}$, which has a reaction barrier in the range 3–4 kcal/mol.^{5,7,8} Several studies also considered the reverse reaction.^{13,17,18} However, to the best of our knowledge, there have been no dynamical studies of the title reactions. There have been a number of studies of the energetics of these

reactions. In addition to the recent work of Sumathi and Nguyen,⁶ in the 1980s Bair et al. performed ab initio calculations, using GVB-CI and POL-CI methods, of various reactions starting from $\text{H} + \text{HCN}$, including H_2CN the global minimum, and two isomers.

Starting the reaction from HCN with H , the standard stationary point analysis⁶ suggests several reactions to consider:



and because of the small barrier, the isomerization



can easily occur. As we will show, there is also a direct pathway from $\text{H} + \text{HCN}$ to *trans*- HCNH^* . In addition, at higher energies, the reaction $\text{H} + \text{HCN} \rightarrow \text{H}_2 + \text{CN}$ can happen; however, this channel is not open at the energies of interest here.

In this paper, we report a high-quality, ab initio global PES of H_2CN system for the ground doublet electronic state. This PES is used in two sets of molecular dynamics calculations of the association reaction probability. One is the quasiclassical trajectory (QCT) method, in which the reactant HCN has zero-point energy. This method is the standard one used in gas-phase reaction dynamics. The second one is the strictly classical trajectory (CT) method, without zero-point energy of the reactant. This method is widely used in condensed phase and/

Received: November 20, 2012

Published: January 10, 2013

Table 1. Comparison of Current Ab Initio (CCSD(T)-F12b/aVDZ) Energies (in kcal/mol relative to H₂ + CN) and Geometries (distances in Å and angles in deg) of Indicated Configurations with Previous Results

H ₂ + CN	r(HH')	r(CN)				energy
ab initio	0.75	1.17				0.0
ref 5 ^a	0.75	1.17				0.0
H ₂ + CN → H + HCN saddle point	r(HH)	r(CH)	r(CN)	α(H'–H–C)	energy	
ab initio	0.79	1.65	1.17	180.0	3.5	
ref 5 ^a	0.79	1.62	1.17	180.0	4.3	
ref 6 ^b	0.80	1.61	1.18	180.0	4.8	
HCN	r(CN)	r(CH)	α(H–C–N)	energy		
ab initio	1.07	1.16	180.0	–23.9		
ref 5 ^a	1.07	1.16	180.0	–23.9 ^b		
H + HCN → H ₂ CN saddle point	r(CN)	r(CH)	r(CH')	α(H–C–N)	α(H'–C–H)	energy
ab initio	1.17	1.07	1.78	161.1	92.1	–17.6
ref 6 ^b	1.18	1.07	1.79	160.3	92.2	–15.2
H ₂ CN	r(CN)	r(CH)	r(CH')	α(H–C–N)	α(H'–C–N)	energy
ab initio	1.25	1.10	1.10	121.1	121.1	–53.9
ref 6 ^b	1.26	1.10	1.10	121.3	121.3	–47.2
H + HCN → <i>cis</i> -HCNH saddle point	r(CN)	r(CH)	r(CH')	α(H–C–N)	α(H'–N–C)	energy
ab initio	1.17	1.07	1.52	167.1	119.5	–13.7
ref 6 ^b	1.18	1.08	1.52	166.5	119.8	–11.8
<i>cis</i> -HCNH	r(CN)	r(CH)	r(CH')	α(H–C–N)	α(H'–N–C)	energy
ab initio	1.23	1.10	1.02	133.8	120.1	–41.2
ref 6 ^b	1.24	1.10	1.03	134.3	118.6	–34.6

^aMRCI(Q) calculation with cc-pVTZ basis. ^bCCSD(T) calculation with 6-311++G(3df,3pd).

or large molecule molecular dynamics simulations. One focus here is the comparison of the threshold energies for the various association reactions using these two methods.

The paper is organized as follows. In Section II, we describe the computational details of the PES, including the ab initio calculations and potential fitting details. Then we show the accuracy of the PES in Section III. In Section IV, QCT and CT calculations are reported for the H + HCN association reactions. Finally, a summary and conclusions are presented in Section V.

II. COMPUTATIONAL DETAILS

Ab Initio Electronic Energy Calculations. The electronic structure calculations were performed using the F12 version of the coupled-cluster singles and doubles excitations with a perturbation treatment of triple excitations, CCSD(T)-F12b,^{20,21} with the aug-cc-pVDZ (aVDZ) basis,^{22,23} as implemented in the MOLPRO²⁴ package.

Here, we are interested in the lowest-lying doublet state. Stationary points on the potential energy surface for the doublet H₂CN has been studied previously using various ab initio methods, including MRCI,⁵ CCSD(T),⁶ and generalized valence bond configuration interaction (GVB-CI).¹ The most accurate results are from the recent CCSD(T) calculations. Selected results from the present calculations are given in Table 1 and compared to previous ab initio results. The present CCSD(T)-F12b calculations give the H₂ + CN ↔ H + HCN reaction barrier of about 3.6 kcal/mol, which is in agreement with the experimental estimate of 3–4 kcal/mol.^{5,7,8} Also, the geometries agree well with previous calculations using MRCI and CCSD(T) methods.

For the generation of data for the PES fitting, the majority of configurations were obtained by running classical direct-dynamics calculations, using density functional theory (B3LYP) with the aVDZ basis, starting from various stationary

points and with a variety of total energies. Preliminary fits were done and then refined by running additional direct-dynamics calculations. Finally, CCSD(T)-F12/aVDZ electronic energies were calculated at roughly 60 000 configurations for the PES fitting.

Fitting the Potential Energy Surface. The potential energy surface of H₂CN system is six dimensional. In addition, the PES should be invariant with respect to permutation of the two H atoms. Thus, we utilize the invariant polynomial method,^{25,26} and expand the expression of PES as follows:

$$V(y_1 \dots y_6) = \sum_{n_1 \dots n_6}^M c_{n_1 \dots n_6} y_1^{n_1} y_6^{n_6} [y_2^{n_2} y_3^{n_3} y_4^{n_4} y_5^{n_5} + y_2^{n_5} y_3^{n_4} y_4^{n_3} y_5^{n_2}]$$

where y_i is Morse-type variable given by $y_i = \exp(-r_i/\lambda)$, with λ fixed at 2.0 bohr, and r_i is the distance between two atoms. Specifically, the internuclear distances are defined as $r_1 = r_{HH'}$, $r_2 = r_{NH'}$, $r_3 = r_{CH'}$, $r_4 = r_{CH}$, $r_5 = r_{NH}$, $r_6 = r_{CN}$. The total power of polynomial is restricted to 7. The coefficients were obtained using standard weighted least-squares fitting, with a cutoff energy of 80 kcal/mol relative to the global minimum energy. After restricting the energy to 80 kcal/mol, there are 59 868 points to be fitted. Weights of points with energies less than 60 kcal/mol equal to 1, from 60 to 70 kcal/mol the weight is 0.7, and above 70 kcal/mol it is 0.5. Figure 1 shows the number of configurations in different energy ranges and the corresponding root-mean-square (RMS) fitting error. Most sampled points are in the energy range from 0 to 60 kcal/mol, and as indicated, the RMS fitting error up to this energy is 0.45 kcal/mol.

III. RESULTS AND DISCUSSION

Properties of the PES. Fifteen stationary points have been reported previously and confirmed in the present work. The comparison of the energies of the stationary points from direct CCSD(T)-F12 ab initio optimization and from the fitted PES is

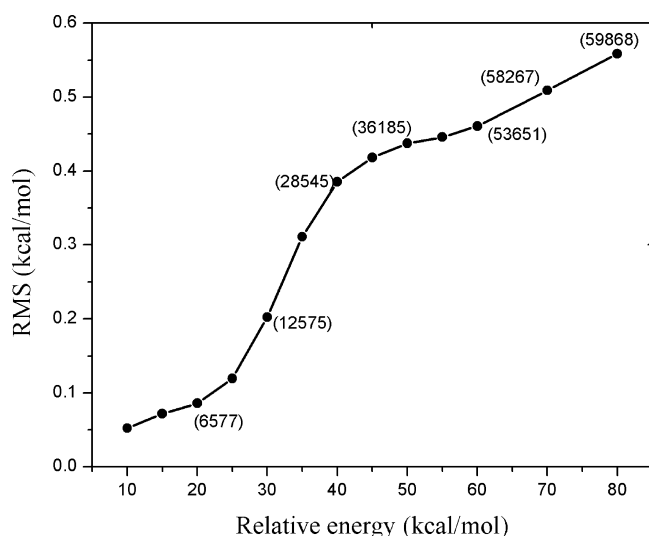


Figure 1. Root-mean-square (RMS) of the PES fitting error as a function of relative energy with respect to the global minimum. The numbers in parentheses are the number of configurations in the energy range.

shown in Figure 2. As seen, the PES achieves very good agreement with the ab initio optimized results. The PES

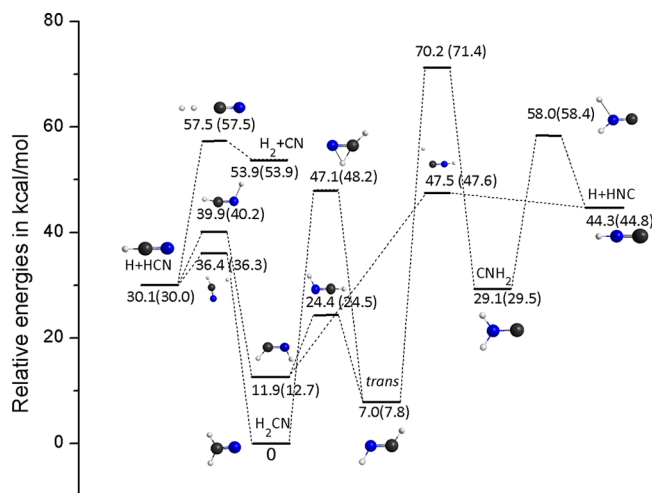


Figure 2. Potential profile of all the stationary points on the PES. The energy outside the parentheses is the energy at the optimized geometry using the PES, and the value in the parentheses corresponds to the optimized results directly from CCSD(T)-F12 calculation.

reaction barrier of $\text{H}_2 + \text{CN} \rightarrow \text{H} + \text{HCN}$ is 3.54 kcal/mol, in good agreement with the ab initio result as well as the deduced experimental value of 3–4 kcal/mol. The barriers for the association reactions R1 and R2 are 6.3 and 9.8 kcal/mol, respectively.

Next, we consider the optimized geometries of selected stationary points and compare with the structures of ab initio results, shown in Table 2. Also, the harmonic frequencies and harmonic zero-point energy (ZPE) associated with the stationary points are given in Table 3. The deviations of the harmonic frequencies and structures obtained from the PES and ab initio computations are quite small.

As seen, the PES is especially accurate for stationary points relevant to the $\text{H}_2 + \text{CN} \leftrightarrow \text{H} + \text{HCN}$ reaction, which we will

study in detail in the future. Several studies have observed that CN is essentially a spectator mode,^{5,18,27,28} demonstrating that CN distance and its vibration state change little during the reaction. A plot of collinear $\text{H} + \text{HCN} \leftrightarrow \text{H}_2 + \text{CN}$ reaction is shown in Figure 3 by varying HH and CH distances and fixing CN distance at equilibrium. As seen, it is quite smooth.

IV. QUASICLASSICAL AND CLASSICAL TRAJECTORY CALCULATIONS

QCT and CT calculations of the $\text{H} + \text{HCN}$ association reactions were performed using the current PES. As usual, we determine whether or not a certain complex is initially formed based on the criterion of three turning points of the distance between the incoming H atom and HCN. The calculations indicate that while it is easy to identify the deep complex H_2CN^* , it is not meaningful to distinguish the *trans/cis*-HCNH isomers, because the interconversion is so rapid. Of course the initial isomer can be identified.

Standard normal-mode sampling²⁹ of the ground vibrational state phase-space of HCN was used in the QCT calculations. For both CT and QCT calculations, the time step is 0.1 fs. The initial distance between H and HCN is 7 Å, and the number of steps we use is 1500. Reaction probabilities are calculated from 2000 trajectories for each impact parameter and collision energy.

As an aid in understanding the results of the QCT and CT calculations, we indicate the energies and barriers of the association reactions from $\text{H} + \text{HCN}$ to H_2CN^* , R1, and *trans/cis*-HCNH*, R2, complexes in Figure 4. The figure also shows the structure of the HCN reactant at the saddle points. As seen, it is bent for both R1 and R2. The standard harmonic vibrationally adiabatic ground state (VAGS) barriers are also given. Recall that these are the saddle point energies plus the associated harmonic ZPEs minus the HCN ZPE. These ZPEs were obtained, as usual, in the harmonic approximation. From many previous dynamics calculations, we know that the VAGS barriers are useful estimates of the quantum and QCT threshold energies. (They are also central to a standard transition state theory treatment of the association rate constant.) There is no rigorous definition of the threshold energy for reaction with barriers. However, we adopt a frequently used one, namely the lowest collision energy where the reaction probability reaches 0.01. Based on many QCT calculations of reactions in the gas phase with barriers, the expectation is that the QCT threshold energy is close to the VAGS barrier. However, often because of a small amount of “zero-point energy leak”, the threshold energies are somewhat lower than this barrier. (Quantum threshold energies are almost always below the VAGS barrier, due to tunneling.) For the CT calculations (with no ZPE), our initial expectation was that the threshold energy for reaction R1 and R2 would be sharp and at the energy of the corresponding saddle point.

The collision energy dependence of the association probabilities of R1 and R2 for QCT and CT calculations for zero impact parameter is shown in Figure 5. First, we focus on the QCT results. As seen, the threshold energy of R1 is about 7 kcal/mol, in good agreement with the VAGS barrier of 7.4 kcal/mol. This also indicates a small amount of ZPE leak, which is a generally known issue in QCT calculation. The observed QCT threshold energy for R2 is roughly 10 kcal/mol, which agrees well with the VAGS barrier of 10.8 kcal/mol.

Next, we investigate the CT results. Recall that in this case HCN is initially fixed at equilibrium geometry, without any

Table 2. Optimized Geometries (distances in Å and angles in deg) of the Indicated Stationary Points from the Fitted PES and Current Ab Initio Calculations

H ₂ + CN		r(HH')	r(CN)					
PES		0.746	1.175					
ab initio		0.746	1.174					
H ₂ + CN → H + HCN saddle point			r(HH)	r(CH)	r(CN)	α(H'–H–C)		
PES		0.790	1.653	1.171	180.0			
ab initio		0.791	1.655	1.170	180.0			
HCN		r(CN)	r(CH)	α(HCN)				
PES		1.069	1.156	180.0				
ab initio		1.069	1.156	180.0				
H + HCN → H ₂ CN saddle point			r(CN)	r(CH)	r(CH')	α(H–C–N)	α(H'–C–H)	α(HCNH')
PES		1.164	1.071	1.816	167.2	88.3	180.0	
ab initio		1.169	1.072	1.779	161.1	92.1	180.0	
H ₂ CN		r(CN)	r(CH)	r(CH')	α(H–C–N)	α(H'–C–N)	α(HCNH')	
PES		1.248	1.098	1.098	120.9	120.9	180.0	
ab initio		1.248	1.097	1.097	121.1	121.1	180.0	
H + HCN → <i>cis</i> -HCNH saddle point			r(CN)	r(CH)	r(CH')	α(H–C–N)	α(H'–N–C)	α(HCNH')
PES		1.172	1.070	1.564	166.2	113.2	0.0	
ab initio		1.172	1.071	1.524	167.1	119.5	0.0	
<i>cis</i> -HCNH		r(CN)	r(CH)	r(CH')	α(H–C–N)	α(H'–N–C)	α(HCNH')	
PES		1.232	1.097	1.024	129.3	116.6	0.0	
ab initio		1.228	1.097	1.025	133.8	120.1	0.0	
<i>trans</i> -HCNH		r(CN)	r(CH)	r(CH')	α(H–C–N)	α(H'–N–C)	α(HCNH')	
PES		1.240	1.098	1.017	122.2	115.4	180.0	
ab initio		1.237	1.095	1.019	124.9	117.6	180.0	

Table 3. Harmonic Vibrational Frequencies ω_i (in cm⁻¹) and Harmonic ZPE (in kcal/mol) of the Indicated Stationary Points from the Fitted PES and Current Ab Initio Calculations

species		ω_1	ω_2	ω_3	ω_4	ω_5	ω_6	ZPE
H ₂ + CN	PES	4383	2046					9.19
	ab initio	4385	2070					9.23
H ₂ + CN → H + HCN saddle point	PES	3268	2141	568(e)	133(e)	−661		9.74
	ab initio	3214	2107	547(e)	106(e)	−676		9.47
HCN	PES	3459	2145	707(e)				10.0
	ab initio	3437	2131	732(e)				10.1
H + HCN → H ₂ CN saddle point	PES	3447	2063	930	740	587	−1020	11.1
	ab initio	3371	2021	910	721	520	−1071	10.8
H ₂ CN	PES	3071	3002	1684	1378	971	930	15.8
	ab initio	3061	2990	1680	1378	975	932	15.9
H + HCN → <i>cis</i> -HCNH saddle point	PES	3407	1997	882	763	502	−1266	10.8
	ab initio	3389	1983	768	699	526	−1473	10.5
<i>cis</i> -HCNH	PES	3585	2909	1737	1165	1141	961	16.4
	ab initio	3346	3004	1803	1034	901	862	15.7
<i>trans</i> -HCNH	PES	3844	3130	1798	1361	1097	954	17.4
	ab initio	3461	3052	1756	1198	977	913	16.2

vibration. Since ZPE is not included in the CT calculation, we expected the threshold energy to be exactly the saddle point energy. However, for both R1 and R2 reactions, the observed threshold energies are significantly higher. For R1, the observed threshold is 12 kcal/mol, which is almost twice as large as the saddle point barrier of 6.3 kcal/mol. The same result appears for R2. For R2, threshold energy of CT is about 13 kcal/mol, much larger than the saddle point barrier of about 9.8 kcal/mol.

To investigate the large differences of threshold energies in the CT and QCT calculations, we consider the reaction R1 in more detail. Specifically, we calculated two relaxed one-dimensional potentials that are of relevance to the QCT and CT reactions. For the QCT calculation, the relevant path is a

fully relaxed one where the potential is minimized as a function of R , the distance of H to the center of mass of HCN. The second path is one where the HCN geometry is fixed at the equilibrium structure. These two paths are shown in Figure 6. As seen, the fully relaxed path connects the reactants to the R1 saddle point and then finally to the H₂CN global minimum. The barrier on this path is the saddle point energy, as expected. The QCT threshold energy is totally consistent with this barrier on this path. As already noted, the HCN reactant is slightly bent at the barrier and this bending is easily achieved using QCT sampling of initial conditions. By contrast, the constrained path displays a ridge at about 12 kcal/mol, which is in good accord with the observed CT threshold energy. Note that

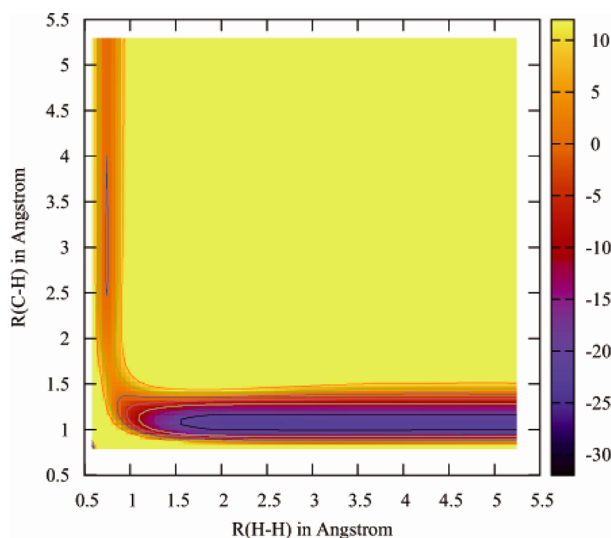


Figure 3. Contour plot of the $\text{H} + \text{HCN} \leftrightarrow \text{H}_2 + \text{CN}$ reaction using the PES (the energy of $\text{H}_2 + \text{CN}$ is set to be zero). The C–H and H–H distances are changed in the plot; the C–N distance is fixed at equilibrium position, and the symmetry is restricted to be collinear.

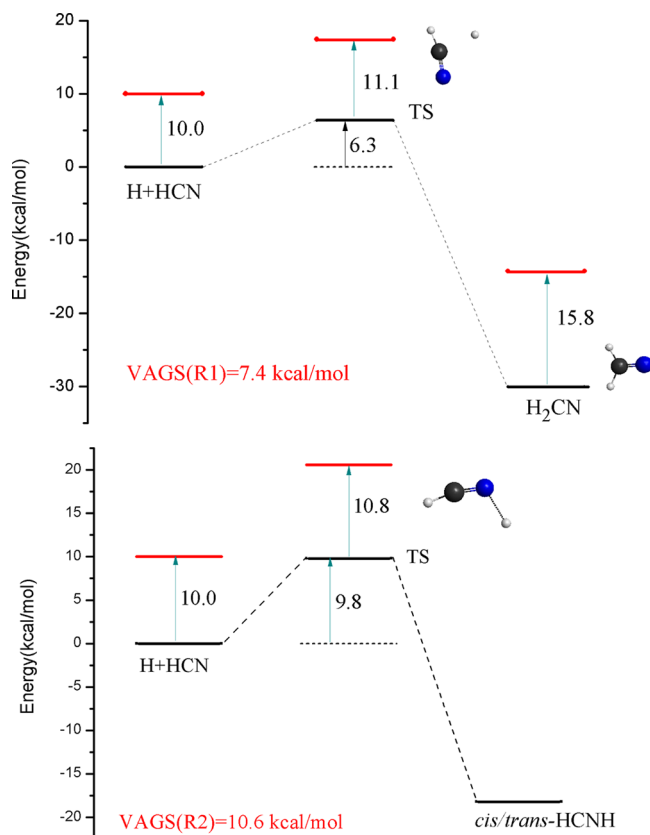


Figure 4. Energies and geometries of the stationary points along the reaction paths of $\text{H} + \text{HCN} \rightarrow \text{H}_2\text{CN}^*$ and cis/trans-HCNH^* on the PES (the energy of $\text{H} + \text{HCN}$ was set to be zero). The red lines indicate the zero-point energies (ZPE).

this ridge develops at a smaller value of R than the saddle point value.

Clearly, in an actual CT trajectory, the H_2CN well is accessed at collision energy above 12 kcal/mol, but we believe this occurs after first visiting this ridge region at roughly 12 kcal/mol. To verify this, we examined a CT trajectory at E_{col} of 13

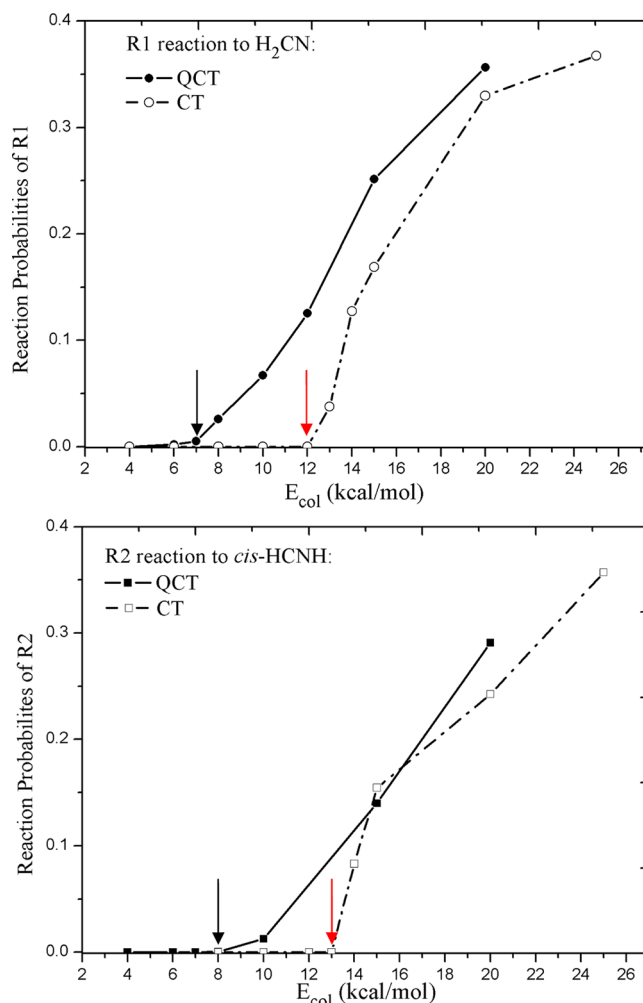


Figure 5. Reaction probabilities of R1 and R2 as a function of collision energy, with impact parameter equal to zero.

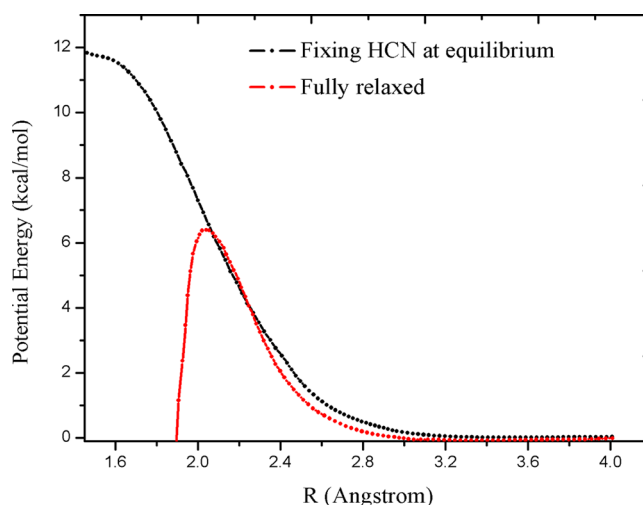


Figure 6. Relaxed potential energy curve for $\text{H}\cdots\text{HCN}$ (the energy of $\text{H} + \text{HCN}$ was set to be zero). R is the distance between H and the center of mass of HCN. For the red curve, the energy is achieved by relaxing all the other internal degrees of freedom. For the black curve, HCN is fixed at the equilibrium configuration, and the angle between H and HCN has been relaxed.

kcal/mol, where the reaction probability of R1 is not zero but small. We monitored $R(t)$, the HCN bond angle, $\theta(t)$, and the potential, $V(t)$, of the CT trajectory, as shown in Figure 7. As

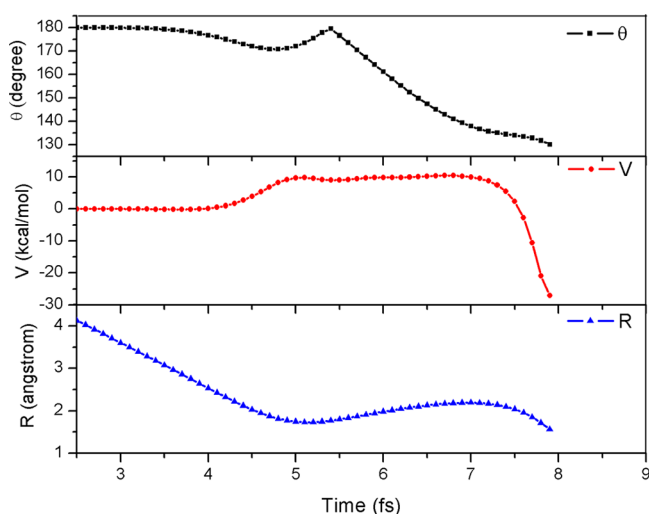


Figure 7. Tracking of classical trajectory (CT) as a function of reaction time at $E_{\text{col}} = 13$ kcal/mol. R is the distance between the incoming H atom and the center of mass (COM) of HCN; V is the potential energy; and θ is the bent angle of HCN.

seen, as R decreases to roughly 3.5 \AA , θ remains at the equilibrium value of 180° . Then, as the H atom approaches, the potential energy increases until it reaches an energy of about 10 kcal/mol, which is smaller than the 12 kcal/mol threshold energy, θ decreases even as the potential remains flat, and R also remains flat. This is the “ridge”. Notice that the value of R at the beginning of the ridge is 1.6 \AA , which is in good agreement with this value at the start of the plateau region of the CT potential cut in Figure 6. After entering the ridge region, there are, not surprisingly, some distortions of the HCN angle and in fact a slight increase in R , as the H_2CN potential well is accessed at roughly 7.5 fs. Based on this result as well as the potential cuts in Figure 6, we assign a critical value of R for reaction to occur for the CT calculations of roughly 1.6 \AA . This is less than the value R at the saddle point, which is roughly 2 \AA .

We can further test these assignments of the critical values of R for the QCT and CT calculations by investigating the reaction probabilities as a function of impact parameter at a collision energy well above the threshold energies. To do this, we use a simple, spherically symmetric textbook model to predict the maximum impact parameter for a reaction with well-defined critical distance for reaction to occur, which we denote generically as R_b . If we make the reasonable assumption that the effective barrier at R_b is the sum of the potential plus the centrifugal potential at R_b , then from the equation $E_{\text{col}} = V_b + b^2 E_{\text{col}} / R_b^2$, where E_{col} is the collision energy, it is trivial to get the following equation for the maximum impact parameter b_{max} for reaction occur (i.e., to surmount the effective barrier). It is

$$b_{\text{max}} = R_b \sqrt{(1 - V_b/E_{\text{col}})}$$

For $E_{\text{col}} \gg V_b$, b_{max} approximately tends to R_b ; however, aside from this limit, we need to know R_b and V_b to predict b_{max} . Application of this simple equation to QCT and CT calculations allows for an immediate qualitative conclusion, which is that $b_{\text{max}}^{\text{QCT}}$ is larger than the $b_{\text{max}}^{\text{CT}}$, where the meaning of the new notations should be obvious. This follows

because R_b is larger and V_b is smaller for QCT than for CT. A quantitative examination of this conclusion is shown in Figure 8

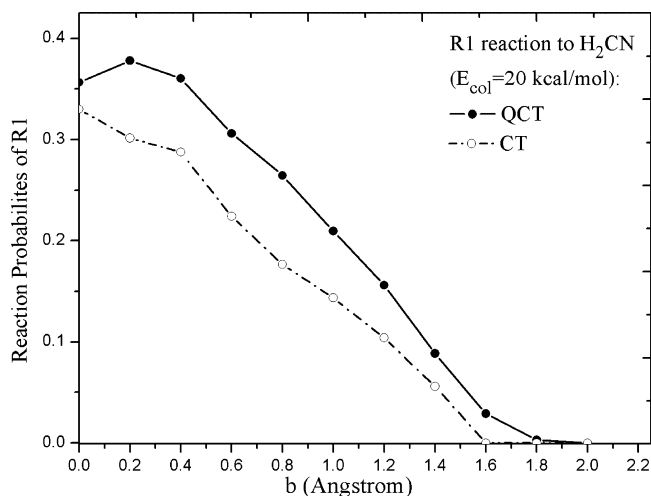


Figure 8. Reaction probabilities of R1 from the CT and QCT calculations as a function of the impact parameter at $E_{\text{col}} = 20$ kcal/mol.

for E_{col} of 20 kcal/mol. First, as seen, $b_{\text{max}}^{\text{CT}}$ is smaller than $b_{\text{max}}^{\text{QCT}}$, as predicted. The latter is roughly 1.8 \AA ; this agrees well with the calculated value of 1.75 \AA from the above equation with the QCT parameters inserted into it. The prediction using CT parameters of 1.6 \AA for R_b and 12 kcal/mol for V_b , is 1.0 \AA , which is not in agreement with observed $b_{\text{max}}^{\text{CT}}$ of 1.6 \AA . This is not surprising, given that instead of a well-defined barrier and critical distance for the CT calculations there is a broad ridge. Thus, while the above equation works quite well for the QCT case, it only works qualitatively well for the CT case. Nevertheless, even a correct qualitative prediction does add further evidence to the conclusion that the CT dynamics is not governed by the saddle point.

We carried out a similar analysis for the addition to the *trans*- and *cis*- isomers of H_2CN and find analogous results. In doing that analysis for the QCT trajectories, we used the geometry and the barrier for the *cis*-saddle point, shown in Figure 4. This barrier does indeed govern the QCT threshold, as noted already. However, when examining QCT trajectories that enter the isomer well, we noticed some trajectories that initially directly formed the *trans* isomer. So, instead of the usual mechanistic picture, that is, where the *cis*-SP is crossed first followed by isomerization to *trans*-HCNH, these trajectories directly formed the *trans* isomer. To investigate this, we determined a relaxed path from the *trans*-minimum to H + HCN. This is shown in Figure 9, along with the corresponding path from the *cis*-minimum. As seen, the two curves are virtually superimposable from the prebarrier region to the asymptotic region. Thus, the labeled “*cis* SP” is evidently the saddle point for both isomers, and thus, the *cis*/*trans* isomerization SP indicated in Figure 2 is largely irrelevant for the association reaction. However, we do note that the isomerization from H_2CN to *trans*-HCNH is difficult because of its high barrier, as seen in Figure 2.

Finally, we note that, at relatively high collision energies of about 15 kcal/mol, we observed trajectories where the two H atoms can exchange. This undoubtedly happens at lower collision energies, too; however, because we did not propagate

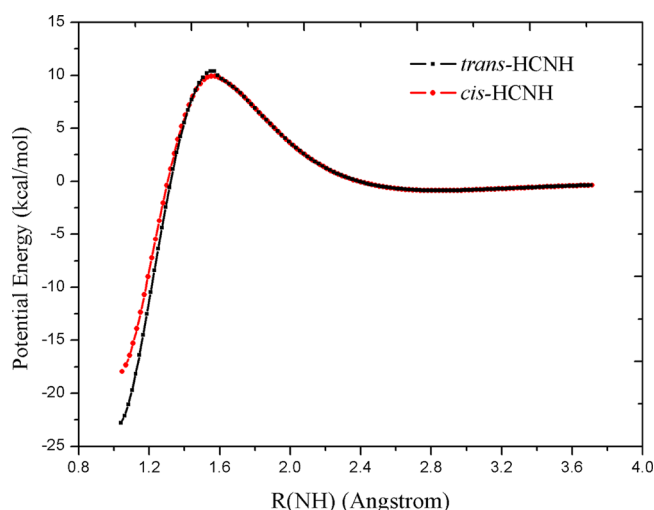


Figure 9. Relaxed potential energy curves from *trans/cis*-HCNH as a function of NH distance (the energy of $\text{H} + \text{HCN}$ was set to be zero). The red curve starts from *cis*-HCNH; the black curve starts from *trans*-HCNH. The NH distance is increased and the energy has been relaxed with respect to all the other internal degrees of freedom.

the trajectories long enough for subsequent dissociation of the energetically excited complexes, we did not observe this.

V. SUMMARY AND CONCLUSIONS

We presented a new ab initio, full-dimensional potential energy surface for the H_2CN system. The PES was constructed by fitting roughly 60 000 CCSD(T)-F12b/aVDZ electronic energies. The permutation of the two H atoms is respected by using the permutationally invariant basis functions in Morse-type variables for the fitting. The PES totally covers 15 stationary points and is especially accurate along the $\text{H}_2 + \text{CN} \rightarrow \text{H} + \text{HCN}$ reaction path. The PES barrier for this reaction is 3.6 kcal/mol, which agrees well with experimental estimates. Also, excellent agreement is achieved for the energies and normal-mode analysis frequencies comparison between the PES and the direct CCSD(T)-F12b calculations.

QCT and CT calculations of the association reactions from $\text{H} + \text{HCN}$ were performed using the PES. We calculated the reaction probabilities of association reactions as a function of the collision energy and the impact parameter. QCT and CT results show large differences in the threshold energy, with CT giving larger threshold energy. In addition, at a given collision energy, the CT calculations give a smaller maximum impact parameter for reaction than the QCT ones. These differences were analyzed in detail, and it was concluded that these differences are due to different barriers of relevance to the QCT and CT calculations. In the case of the QCT calculations, the saddle point barrier is the relevant barrier. This is the usual QCT result, consistent with many QCT calculations of reaction dynamics. The new result is the significantly higher threshold energy seen in the CT calculations.

For this polyatomic reaction, the origin of this difference is evidently the distorted geometry of the reactant HCN at the saddle point. In the CT calculations, with no initial zero-point energy, HCN evidently remains collinear during the approach to the saddle point and does not distort to “in time” to achieve the SP geometry. By contrast, the QCT calculation, with initial ZPE in the HCN, does sample bent configuration of the HCN and thus accessing the SP geometry does occur easily. The fact

indicates the importance of including the ZPE in reaction dynamics studies. In addition, the reaction channel from $\text{H} + \text{HCN}$ directly to *trans*-HCNH is discussed in detail for the first time, which shows the same saddle point with the reaction to *cis*-HCNH.

AUTHOR INFORMATION

Corresponding Author

*E-mail: jmbowma@emory.edu

Notes

The authors declare no competing financial interest.

ACKNOWLEDGMENTS

We thank NASA for financial support through Grant No. NNX12AF42G from the NASA Astrophysics Research and Analysis program.

REFERENCES

- (1) Bair, R. A.; Dunning, T. H. Theoretical studies of the reactions of HCN with atomic hydrogen. *J. Chem. Phys.* **1985**, *82*, 2280–2294.
- (2) Wagner, A. F.; Bair, R. A. An ab initio determination of the rate constant for $\text{H}_2 + \text{CN} \rightarrow \text{H} + \text{HCN}$. *Int. J. Chem. Kinet.* **1986**, *18*, 473–486.
- (3) Sun, Q.; Bowman, J. M. Reduced dimensionality quantum reactive scattering: $\text{H}_2 + \text{CN} \rightarrow \text{H} + \text{HCN}$. *J. Chem. Phys.* **1990**, *92*, 5201–5210.
- (4) Sun, Q.; et al. Experimental and reduced dimensionality quantum rate coefficients for $\text{H}_2(\text{D}_2) + \text{CN} \rightarrow \text{H}(\text{D})\text{CN} + \text{H}(\text{D})$. *J. Chem. Phys.* **1990**, *93*, 4730–4739.
- (5) Horst, M. A.; et al. Potential energy surface and quasiclassical trajectory studies of the $\text{CN} + \text{H}_2$ reaction. *J. Chem. Phys.* **1996**, *105*, 558–571.
- (6) Sumathi, R.; Nguyen, M. T. A theoretical study of the CH_2N system: Reactions in both lowest lying doublet and quartet states. *J. Phys. Chem. A* **1998**, *102*, 8013–8020.
- (7) Wang, J. H.; et al. Experimental and theoretical angular and translational energy distributions for the reaction $\text{CN} + \text{D}_2 \rightarrow \text{DCN} + \text{D}$. *J. Chem. Phys.* **1997**, *107*, 7869–7875.
- (8) Zhu, W.; et al. Quantum dynamics study of $\text{H}_2 + \text{CN} \rightarrow \text{HCN} + \text{H}$ reaction in full dimensions. *J. Chem. Phys.* **1998**, *108*, 3509–3516.
- (9) Nguyen, M. T.; et al. Another look at the decomposition of methyl azide and methanimine: How is HCN formed? *J. Phys. Chem.* **1996**, *100*, 6499–6503.
- (10) Kaledin, A. L.; et al. Potential energy surface and vibrational eigenstates of the $\text{H}_2\text{-CN}(\text{X}^2\Sigma^+)$ van der Waals complex. *J. Chem. Phys.* **1999**, *110*, 10380–10392.
- (11) Takayanagi, T. Quantum reactive scattering calculation for four-atom chemical reaction systems—Application of a fixed-angle approximation. *Bull. Chem. Soc. Jpn.* **1995**, *68*, 2527–2532.
- (12) Carter, S.; et al. Ab initio calculations of force fields for H_2CN and ClHCN and vibrational energies of H_2CN . *Spectrochim. Acta A* **1997**, *53*, 1179–1188.
- (13) Troya, D.; et al. A quasiclassical trajectory study of the $\text{H} + \text{HCN} \rightarrow \text{H}_2 + \text{CN}$ reaction dynamics. *J. Chem. Phys.* **2000**, *113*, 6253.
- (14) Miller, J. A.; Bowman, C. T. Mechanism and modeling of nitrogen chemistry in combustion. *Prog. Energy Combust.* **1989**, *15*, 287–338.
- (15) Guo, Y.; et al. Interpolating moving least-squares methods for fitting potential energy surfaces: An application to the H_2CN unimolecular reaction. *J. Chem. Phys.* **2007**, *126*, 104105.
- (16) Coletti, C.; Billing, G. D. Quantum-classical calculation of cross sections and rate constants for the $\text{H}_2 + \text{CN} \rightarrow \text{HCN} + \text{H}$ reaction. *J. Chem. Phys.* **2000**, *113*, 11101–11108.
- (17) Lambert, H. M.; et al. Cross sections and energy disposal for cyanogen(X) produced in the hydrogen atom + hydrogen cyanide reaction at 53 and 58 kcal mol⁻¹ collision energies. *J. Phys. Chem.* **1993**, *97*, 128.

- (18) Johnston, G. W.; Bersohn, R. Energy-Distribution of the CN Products of the $\text{H} + \text{HCN}$, $\text{H} + \text{ClCN}$, and $\text{F} + \text{HCN}$ Reactions. *J. Chem. Phys.* **1989**, *90*, 7096–7102.
- (19) Sims, I. R.; Smith, I. W. M. Rate constants for the reactions $\text{CN}(\nu = 0)$, $\text{CN}(\nu = 1) + \text{H}_2$, $\text{D}_2 \rightarrow \text{HCN}$, $\text{DCN} + \text{H}$, D between 295 and 768 K, and comparisons with transition state theory calculations. *Chem. Phys. Lett.* **1988**, *149*, 565–571.
- (20) Adler, T. B.; et al. A simple and efficient CCSD(T)-F12 approximation. *J. Chem. Phys.* **2007**, *127*, 221106.
- (21) Knizia, G.; et al. Simplified CCSD(T)-F12 methods: Theory and benchmarks. *J. Chem. Phys.* **2009**, *130*, 054104.
- (22) Dunning, T. H. Gaussian-basis sets for use in correlated molecular calculations. I. The atoms boron through neon and hydrogen. *J. Chem. Phys.* **1989**, *90*, 1007–1023.
- (23) Kendall, R. A.; et al. Electron affinities of the 1st-row atoms revisited—Systematic basis sets and wave functions. *J. Chem. Phys.* **1992**, *96*, 6796–6806.
- (24) Werner, H. J.; Knizia, G.; Mandy, F. R.; Schütz, M.; Celani, P.; Korona, T.; Lindh, R.; Mitrushenkov, A.; Rauhut, G.; Shamasundar, K. R.; Adler, T. B.; et al. *MOLPRO*; University College Cardiff Consultants Ltd.: Cardiff, U.K., 2008. <http://www.molpro.net>
- (25) Bowman, J. M.; et al. High-dimensional ab initio potential energy surfaces for reaction dynamics calculations. *Phys. Chem. Chem. Phys.* **2011**, *13*, 8094.
- (26) Braams, B. J.; Bowman, J. M. Permutationally invariant potential energy surfaces in high dimensionality. *Int. Rev. Phys. Chem.* **2009**, *28*, 577–606.
- (27) Pfeiffer, J. M.; et al. Reactions of O, H, and Cl atoms with highly vibrationally excited HCN: Using product states to determine mechanisms. *J. Chem. Phys.* **1996**, *104*, 4490–4501.
- (28) Kreher, C.; et al. State-to-state reaction dynamics of $\text{R} + \text{HCN}(\nu_1 \nu_2^h \nu_3) \rightarrow \text{RH} + \text{CN}(\nu, J)$ with $\text{R} = \text{Cl}, \text{H}$. *J. Chem. Phys.* **1996**, *104*, 4481–4489.
- (29) Hase, W. L. Classical trajectory simulations: Initial conditions. In *Encyclopedia of Computational Chemistry*; Allinger, N. L., Ed.; Wiley: New York, 1998; Vol. 1, pp 402–407.